High-order QED Contribution to Electron and Muon $g-2$

T. Aoyama (KEK)

based on collaboration with
T. Kinoshita (Cornell and UMass Amherst),
M. Nio (RIKEN),
M. Hayakawa (Nagoya University)

December 16–19, 2019

QUCS 2019

YITP, Kyoto

Anomalous magnetic moment of leptons

- Electrons and Muons have magnetic moment along their spins, given by

$$\vec{\mu} = g \frac{e\hbar}{2m} \vec{s}$$

It is known that g-factor deviates from Dirac's value ($g = 2$), and it is called Anomalous magnetic moment

$$a_\ell \equiv (g-2)/2$$

It is much precisely measured for electron and muon.

- Electron $g-2$ is explained almost entirely by QED interaction between electron and photons. It has been the most stringent test of QED and the standard model.

- Muon $g-2$ is more sensitive to high energy physics, and thus a window to new physics beyond the standard model.

Anomalous magnetic moment of electron

- The precise measurements of electron and positron $g-2$ have been carried out using Penning trap. Earlier measurement by Univ. of Washington group:

$$a_{e^-}(\text{UW87}) = 1\;159\;652\;188.4\;(43) \times 10^{-12} \qquad [3.7\text{ppb}]$$

$$a_{e^+}(\text{UW87}) = 1\;159\;652\;187.9\;(43) \times 10^{-12} \qquad [3.7\text{ppb}]$$

Van Dyck, Schwinberg, Dehmelt, PRL59, 26 (1987)

- The best measurement of electron $g-2$ is obtained by Harvard group, using cylindrical Penning trap and quantum jump spectroscopy:

$$a_e(\text{HV08}) = 1\;159\;652\;180.73\;(28) \times 10^{-12} \qquad [0.24\text{ppb}]$$

Hanneke, Fogwell, Gabrielse, PRL100, 120801 (2008)
Hanneke, Fogwell Hoogerheide, Gabrielse, PRA83, 052122 (2011)

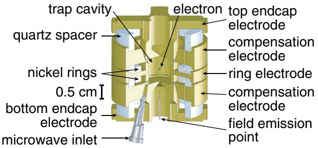

FIG. 2 (color). Cylindrical Penning trap cavity used to confine a single electron and inhibit spontaneous emission.

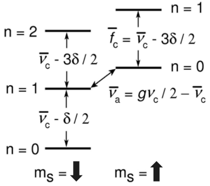

- Further improvement of electron anomaly as well as new measurement of positron is ongoing.

Gabrielse, Fayer, Myers, Fan, Atoms **7** 45 (2019)

Anomalous magnetic moment of muon

- Experiments using muon storage ring started at CERN in 1960's. The latest experiment was conducted at BNL in E821 experiment.

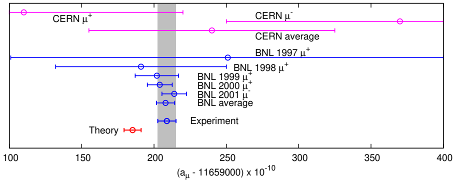

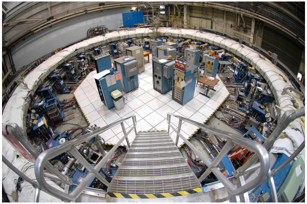

- Latest world average of the measured a_μ:

$$a_\mu[\text{exp}] = 116\,592\,089\,(63) \times 10^{-11} \qquad [0.54\text{ppm}]$$

Bennett, et al., Phys. Rev. D73, 072003 (2006)
Roberts, Chinese Phys. C 34, 741 (2010)

- New experiments are on-going at FermiLab and J-PARC, expecting $\mathcal{O}(0.1)$ ppm.

Muon g-2 collaboration (Grange et al.), arXiv:1501.06858 (2015)
Muon g-2/EDM at J-PARC (Abe et al.), PTEP 053C02 (2019)

Standard Model prediction of a_e

- Contributions to electron $g-2$ within the context of the standard model consist of:

$$a_e = a_e(QED) + a_e(Hadronic) + a_e(Weak)$$

- QED contribution is further divided according to its lepton-mass dependence through mass-ratio:

$$a_e(\mathrm{QED}) = \underbrace{A_1}_{e,\gamma} + \underbrace{A_2(m_e/m_\mu)}_{e,\mu,\gamma} + \underbrace{A_2(m_e/m_\tau)}_{e,\tau,\gamma} + \underbrace{A_3(m_e/m_\mu, m_e/m_\tau)}_{e,\mu,\tau,\gamma}$$

- Each contribution is evaluated by perturbation theory:

$$A_i = A_i^{(2)}\left(\frac{\alpha}{\pi}\right) + A_i^{(4)}\left(\frac{\alpha}{\pi}\right)^2 + A_i^{(6)}\left(\frac{\alpha}{\pi}\right)^3 + A_i^{(8)}\left(\frac{\alpha}{\pi}\right)^4 + \cdots$$

These coefficients are calculated by using Feynman-diagram techniques.

Note that

$$\left(\frac{\alpha}{\pi}\right)^4 \simeq 29.1 \times 10^{-12}, \qquad \left(\frac{\alpha}{\pi}\right)^5 \simeq 0.07 \times 10^{-12}.$$

QED contribution: Diagrams

- There is one vertex diagram contributing to 2nd order term: 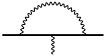
- 4th order term comes from 7 Feynman diagrams:

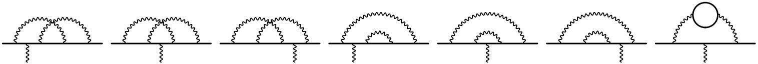

- 6th order term receives contributions from 72 Feynman diagrams, represented by these five types:

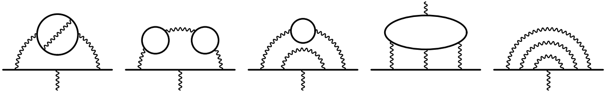

- There are 891 Feynman diagrams contributing to 8th order term. They are classified into 13 gauge-invariant groups.

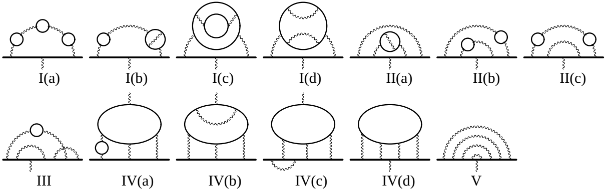

QED contribution: Summary

Coefficient $A_i^{(2n)}$	Value (Error)	References
$A_1^{(2)}$	0.5	Schwinger 1948
$A_1^{(4)}$	$-0.328\,478\,965\,579\,193\cdots$	Petermann 1957, Sommerfield 1958
$A_2^{(4)}(m_e/m_\mu)$	$0.519\,738\,676\,(24)\times10^{-6}$	Elend 1966
$A_2^{(4)}(m_e/m_\tau)$	$0.183\,790\,(25)\times10^{-8}$	Elend 1966
$A_1^{(6)}$	$1.181\,241\,456\,587\cdots$	Laporta-Remiddi 1996, Kinoshita 1995
$A_2^{(6)}(m_e/m_\mu)$	$-0.737\,394\,164\,(24)\times10^{-5}$	Samuel-Li, Laporta-Remiddi, Laporta
$A_2^{(6)}(m_e/m_\tau)$	$-0.658\,273\,(79)\times10^{-7}$	Samuel-Li, Laporta-Remiddi, Laporta
$A_3^{(6)}(m_e/m_\mu, m_e/m_\tau)$	$0.1909\,(1)\times10^{-12}$	Passera 2007
$A_1^{(8)}$	$-1.912\,245\,764\cdots$	Laporta 2017, AHKN 2015
$A_2^{(8)}(m_e/m_\mu)$	$0.916\,197\,070\,(37)\times10^{-3}$	Kurz et al 2014, AHKN 2012
$A_2^{(8)}(m_e/m_\tau)$	$0.742\,92\,(12)\times10^{-5}$	Kurz et al 2014, AHKN 2012
$A_3^{(8)}(m_e/m_\mu, m_e/m_\tau)$	$0.746\,87\,(28)\times10^{-6}$	Kurz et al 2014, AHKN 2012
$A_1^{(10)}$	$6.737\,(159)$	AKN 2018,2019
$A_2^{(10)}(m_e/m_\mu)$	$-0.003\,82\,(39)$	AHKN 2012,2015
$A_2^{(10)}(m_e/m_\tau)$	$\mathcal{O}(10^{-5})$	
$A_3^{(10)}(m_e/m_\mu, m_e/m_\tau)$	$\mathcal{O}(10^{-5})$	

All terms up to 8th order are well-known. 10th order term is obtained numerically.

QED contribution: 8th order term

- Mass-independent term $A_1^{(8)}$
  - Near-analytic very precise result by Laporta (up to 1100 digits)
    $-1.9122457649264455741526471674\ldots$ Laporta, PLB772, 232 (2017)
  - Alternative semi-analytic result
    $-1.87(12)$ Marquad et al, arXiv:1708.07138
  - Numerical result
    $-1.91298(84)$ AHKN, PRL109, 111809 (2012); PRD91, 033006 (2015)
- Mass-dependent terms $A_2^{(8)}$ and $A_3^{(8)}$
  - Numerical evaluation. AHKN, PRL109, 111809 (2012)
  - Analytic calculation by the series expansion in mass-ratio $m_e/m_\ell \ll 1$.
    Kurz et al. PRD93, 053017 (2016)

	Analytic	Numerical
$A_2^{(8)}(m_e/m_\mu)$	$0.916\,197\,070\,(37) \times 10^{-3}$	$0.9222\,(66) \times 10^{-3}$
$A_2^{(8)}(m_e/m_\tau)$	$0.742\,92\,(12) \times 10^{-5}$	$0.738\,(12) \times 10^{-5}$
$A_3^{(8)}(m_e/m_\mu, m_e/m_\tau)$	$0.746\,87\,(28) \times 10^{-6}$	$0.7465\,(18) \times 10^{-6}$

- Now the 8th order term is well-known.

QED contribution: 10th order term

- Numerical evaluation of the complete 10th order contribution was reported in 2012 and an updated result was published in 2015. Latest value is:

  $$A_1^{(10)} = 6.737\ (159)$$

- Contribution to $A_1^{(10)}$ mainly comes from Set V that consists of 6354 vertex diagrams without closed lepton loops.

  Recently, Volkov announced their result by an independent numerical method.

  $$A_1^{(10)}[\text{Set V}] = \begin{cases} 7.668\ (159) & \text{AKN, Atoms, 7, 28 (2019)} \\ 6.793\ (90) & \text{Volkov, PRD100, 096004 (2019)} \end{cases}$$

  Difference $-0.87\ (18)\ [4.8\sigma]$ does not affect seriously in the current precision.

- Mass-dependent term is also evaluated:

  $$A_2^{(10)}(m_e/m_\mu) = -0.003\,82\ (39)$$

  tau-lepton contribution is negligibly small for the current experimental precision.

Fine Structure Constant α

- To obtain the theoretical prediction of a_e, we need a value of the fine-structure constant α determined independent of QED.

- Two high-precision values of α are obtained from the measurement of $h/m(X)$ of the Rb and Cs by the atom interferometer through the relation:

$$\alpha^{-1} = \left[\frac{2R_\infty}{c}\frac{A_r(X)}{A_r(e)}\frac{h}{m(X)}\right]^{-1/2}$$

where

- R_∞ the Rydberg constant
- $A_r(X)$ relative atomic mass of an atom X
- $m(X)$ mass of an atom X

It leads to

$$\alpha^{-1}(\mathrm{Rb}) = 137.035\,998\,995\,(85)\;[0.62\mathrm{ppb}]$$ Bouchendira et al, PRL106, 080801 (2011)

$$\alpha^{-1}(\mathrm{Cs}) = 137.035\,999\,046\,(27)\;[0.20\mathrm{ppb}]$$ Parker et al, Science, 360, 191 (2018)

Theoretical Prediction of a_e

- Using α(Cs) and including the hadronic and weak contributions, the theoretical prediction of a_e becomes:

QED	mass-independent	mass-dependent	sum
2nd	1 161 409 733.21 (23)	0	1 161 409 733.21 (23)
4th	−1 772 305.063 85 (70)	2.814 1613 (13)	−1 772 302.249 69 (70)
6th	14 804.203 6740 (88)	−0.093 240 76 (10)	14 804.110 4333 (88)
8th	−55.667 989 379 (44)	0.026 909 719 (35)	−55.641 079 660 (56)
10th	0.456 (11)	−0.000 258 (26)	0.455 (11)
a_e(QED)	1 159 652 177.14 (23)	2.747 5720 (14)	1 159 652 179.88 (23)
Weak			
a_e(weak)			0.030 53 (23)
Hadron			
VP LO			1.849 (10)
VP NLO			−0.2213 (11)
VP NNLO			0.027 99 (17)
LbyL			0.037 (5)
a_e(hadron)			1.693 (12)
a_e(theory)			1 159 652 181.61 (23)

Theoretical Prediction of a_e

- We obtain the theoretical prediction of a_e as

$$a_e(\text{theory: } \alpha(\text{Rb})) = 1\ 159\ 652\ 182.037\ (720)(11)(12) \times 10^{-12}$$
$$a_e(\text{theory: } \alpha(\text{Cs})) = 1\ 159\ 652\ 181.606\ (229)(11)(12) \times 10^{-12}$$

where uncertainties are due to fine-structure constant α, QED 10th order, and hadronic contribution.

- The measurement of a_e is

$$a_e(\text{expt.}) = 1\ 159\ 652\ 180.73\ (28) \times 10^{-12}$$

- The differences between theory and measurement are

$$a_e(\text{expt.}) - a_e(\text{theory: } \alpha(\text{Rb})) = -1.31\ (77) \times 10^{-12}\ [1.7\sigma]$$
$$a_e(\text{expt.}) - a_e(\text{theory: } \alpha(\text{Cs})) = -0.88\ (36) \times 10^{-12}\ [2.4\sigma]$$

Muon $g-2$: QED contribution

- What distinguishes a_e(QED) and a_μ(QED) is the mass-dependent component.
- Light lepton loop contribution yields large logarithmic enhancement involving a factor $\ln(m_e/m_\mu)$.
  - Vacuum polarization loop:

$$\frac{2}{3}\ln(m_\mu/m_e) - \frac{5}{9} \simeq 3.$$

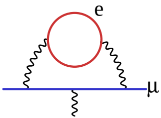

  - Light-by-light scattering loop:

$$\frac{2}{3}\pi^2 \ln(m_\mu/m_e) \simeq 35.$$

6th-order l-by-l effect is important.

c.f. Aldins, Kinoshita, Brodsky, Dufner, PRL8, 441 (1969)

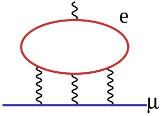

- Therefore, the sets of diagrams giving the leading contribution can be identified and were evaluated in the earlier stage.
  The entire contribution including non-leading diagrams have been evaluated.

Muon $g-2$: QED contribution

- a_μ(QED) is known up to 10th order. Their values contributing to mass-dependent terms are:

	$A_2(m_\mu/m_e)$	$A_2(m_\mu/m_\tau)$	$A_3(m_\mu/m_e, m_\mu/m_\tau)$
4th	1.094 258 3093 (76)	0.000 078 076 (11)	—
6th	22.868 379 98 (20)	0.000 360 671 (94)	0.000 527 738 (75)
8th	132.685 2 (60)	0.042 4941 (53)	0.062 722 (10)
10th	742.32 (86)	$-$0.0656 (45)	2.011 (10)

Elend, PL20, 682 (1966); Samuel and Li, PRD44, 3935 (1991); Li, Mendel and Samuel, PRD47, 1723 (1993)
Laporta, Nuovo Cim. A106, 675 (1993); Laporta and Remiddi, PLB301, 440 (1993); Czarnecki and Skrzypek, PLB449, 354 (1999)
Laporta, PLB312, 495 (1993); Kinoshita and Nio, PRD70, 113001 (2004); Kurz, Liu, Marquard, Steinhauser, NPB879, 1 (2014)
Laporta, PLB328, 522 (1994); Kinoshita and Nio, PRD73, 053007 (2006)
TA, Hayakawa, Kinoshita, Nio, Watanabe, PRD78, 053005 (2008)
TA, Asano, Hayakawa, Kinoshita, Nio, Watanabe, PRD81, 053009 (2010)
TA, Hayakawa, Kinoshita, Nio, PRD78, 113006 (2008); 82, 113004 (2010); 83, 053002 (2011)
83, 053003 (2011); 84, 053003 (2011); 85, 033007 (2012); 85, 093013 (2012)

- Together with the mass-independent term A_1, we obtain:

$$a_\mu(\mathrm{QED} : \alpha(\mathrm{Cs})) = 116\,584\,718.931\ (7)\ (17)\ (6)\ (100)\ (23)\ [104] \times 10^{-11}$$

$$a_\mu(\mathrm{QED} : \alpha(a_e)) = 116\,584\,718.842\ (7)\ (17)\ (6)\ (100)\ (28)\ [106] \times 10^{-11}$$

(mass ratio)(8th)(10th)(12th)(α)[combined]

Muon $g-2$: theory

- The standard model contributions are summarized as follows: (in unit of 10^{-10})

	KNT19	DHMZ19	J18
a_μ(had. vp. LO)	692.78 ± 2.42	693.9 ± 4.0	688.07 ± 4.14
a_μ(had. vp. NLO)	-9.83 ± 0.04	-9.87 ± 0.01	-9.93 ± 0.07
a_μ(had. vp. NNLO)	1.24 ± 0.01	1.24 ± 0.01	1.22 ± 0.01
a_μ(had. LbL)	10.5 ± 2.6		
a_μ(weak)	15.36 ± 0.10		
a_μ(QED)	$11\,658\,471.89 \pm 0.01$		

Keshavarzi, Nomura, Teubner, arXiv:1911.00367
Davier, Hoecker, Malaescu, Zhang, arXiv:1908.00921
Jegerlehner, EPJ Web Conf. 166, 00022 (2018)
Prades, de Rafael, Vainshtein, Adv. Ser. Direct. High Energy Phys. 20, 303 (2009)
Czarnecki, Marciano, Vainshtein, PRD67, 073006 (2003)
Gnendiger, Stöckinger, Stöckinger-Kim, PRD88, 053005 (2013)
Ishikawa, Nakazawa, Yasui, PRD99, 073004 (2019)

- The standard model prediction of muon $g-2$:

		$a_\mu^{\text{exp}} - a_\mu^{\text{SM}}$
$11\,659\,181.1 \pm 3.8 \times 10^{-10}$	KNT19	27.1 ± 7.3 [3.7σ]
$11\,659\,183.0 \pm 4.8 \times 10^{-10}$	DHMZ19	26.1 ± 7.9 [3.3σ]
$11\,659\,177.6 \pm 4.4 \times 10^{-10}$	J18	31.3 ± 7.7 [4.1σ]
$11\,659\,208.9 \pm 6.3 \times 10^{-10}$	exp	

Muon $g-2$: theory

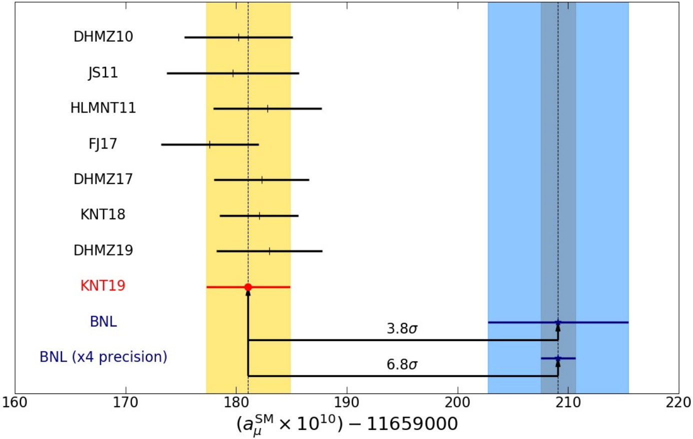

Keshavarzi, Nomura, Teubner, arXiv:1911.00367

Numerical evaluation of QED 10th order term

- 12 672 Feynman diagrams contribute to 10th order term.
  They are classified into 32 gauge invariant sets within 6 supersets.

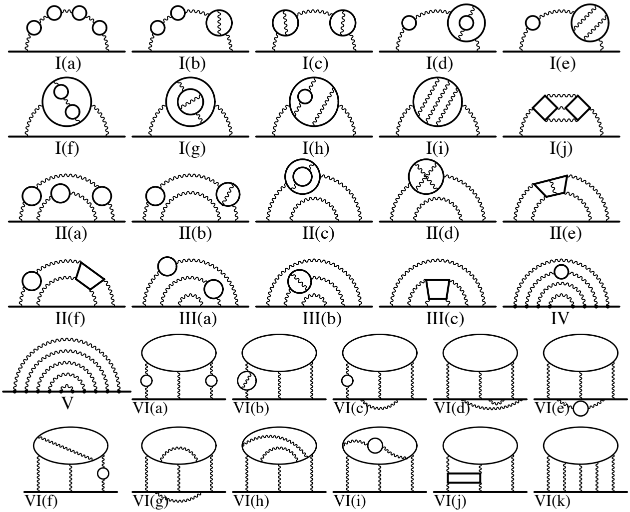

Most difficult is Set V that consists of 6354 diagrams w/o lepton loops.

Magnetic moment contribution

- Magnetic property of lepton can be studied through examining its scattering by a static magnetic field.
  The amplitude can be represented as:

$$e\bar{u}(p'')\left[\gamma^{\mu} F_1(q^2) + \frac{i}{2m}\sigma^{\mu\nu} q_{\nu} F_2(q^2)\right] u(p') A^{e}_{\mu}(\vec{q})$$

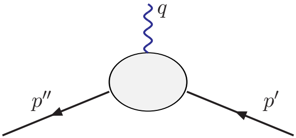

- The anomalous magnetic moment is the static limit of the magnetic form factor $F_2(q^2)$:

$$a_{\ell} = F_2(0) = Z_2 M, \qquad M = \lim_{q^2 \to 0} \mathrm{Tr}(P_{\nu}(p,q)\Gamma^{\nu})$$

  where Γ^{ν} is the proper vertex function with the external lepton on the mass shell, and $P_{\nu}(p,q)$ is the magnetic projection operator.

Numerical Approach

- Amplitude is given by an integral over loop momenta according to Feynman-Dyson rule.
  It is converted into Feynman parametric integral over $\{z_i\}$. Momentum integration is carried out analytically that yields

$$M_{\mathcal{G}}^{(2n)} = \left(-\frac{1}{4}\right)^n \Gamma(n-1) \int (dz)_{\mathcal{G}} \left[\frac{F_0}{U^2 V^{n-1}} + \frac{F_1}{U^3 V^{n-2}} + \cdots \right]$$

- Integrand is expressed by a rational function of terms called *building blocks*, U, V, B_{ij}, A_j, and C_{ij}.
  Building blocks are given by functions of $\{z_i\}$, reflecting the topology of diagram, flow of momenta, etc.

- A set of vertex diagrams Λ obtained by inserting an external vertex into each lepton line of self-energy diagram Σ can be related by Ward-Takahashi identity.

$$\Lambda^\nu(p,q) \simeq -q_\mu \left. \frac{\partial \Lambda^\mu(p,q)}{\partial q_\nu} \right|_{q\to 0} - \frac{\partial \Sigma(p)}{\partial p_\nu}.$$

  For 10th order Set V, the number of independent integrals reduces to 1/9.

Subtraction of UV Divergences

- UV divergence occurs when loop momenta in a subdiagram go to infinity. It corresponds to the region of Feynman parameter space $z_i \sim \mathcal{O}(\epsilon)$ for $i \in \mathcal{S}$.

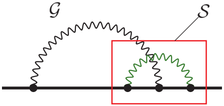

- In order to carry out subtraction numerically, the singularities are cancelled point-by-point on Feynman parameter space.

$$M_{\mathcal{G}} - L_{\mathcal{S}} M_{\mathcal{G}/\mathcal{S}} \quad \longrightarrow \quad \int (dz)_{\mathcal{G}} \left[m_{\mathcal{G}} - \mathbb{K}_{\mathcal{S}} m_{\mathcal{G}} \right]$$

- The subtraction integrand $\mathbb{K}_{\mathcal{S}} m_{\mathcal{G}}$ is derived from $m_{\mathcal{G}}$ by simple power-counting rule called ***K*-operation**. Cvitanović and Kinoshita, 1974
- By construction, subtraction terms can be factorized into (UV-divergent part of) renormalization constant and lower-order magnetic part.

$$\int (dz)_{\mathcal{G}} \left[\mathbb{K}_{\mathcal{S}} m_{\mathcal{G}} \right] \quad = \quad L_{\mathcal{S}}^{\text{UV}} M_{\mathcal{G}/\mathcal{S}}$$

$L_{\mathcal{S}}^{\text{UV}}$ is the leading UV-divergent part of $L_{\mathcal{S}}$.

IR subtraction Scheme

- A diagram may have IR divergence when some momenta of photon go to zero. It is really divergent by “enhancer” leptons that are close to on-shell by kinematical constraint.

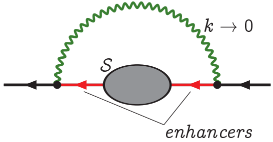

- We adopt subtraction approach for these divergences point-by-point on Feynman parameter space.

- There are two types of sources of IR divergence in $M_{\mathcal{G}}$ associated with a self-energy subdiagram. To handle these divergences, we introduce two subtraction operations:
  - ***R*-subtraction** to remove the residual self-mass term

    $$\mathbb{R}_{\mathcal{S}} M_{\mathcal{G}} = \widetilde{\delta m}_{\mathcal{S}} M_{\mathcal{G}/\mathcal{S}(i^*)}$$

  - ***I*-subtraction** to subtract remaining logarithmic IR divergence

    $$\mathbb{I}_{\mathcal{S}} M_{\mathcal{G}} = \widetilde{L}_{\mathcal{G}/\mathcal{S}(k)} M_{\mathcal{S}}$$

Step-by-step example with 4th-order diagrams : Step 1

- Let us illustrate the steps by simpler case,
  e.g. 4th-order diagrams.
- There are 7 diagrams of 4th order;
  6 of them have no closed lepton loop (q-type).
- They are *WT-sum*ed into 2 self-energy-like diagrams, 4a and 4b.

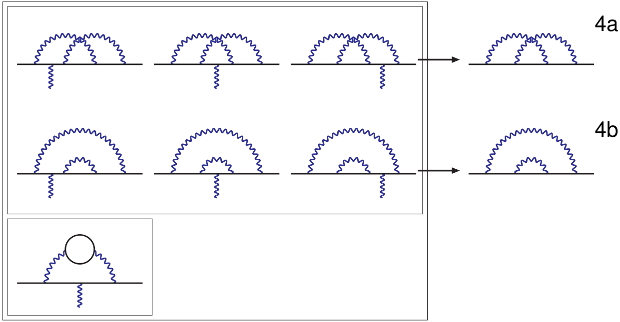

Step 2: Amplitude

- Introduce Feynman parameters $z_1, \dots, z_5$ to propagators:

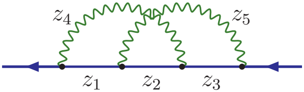

- Anomalous magnetic moment M_{4a} is converted analytically into the form:

$$M_{4a} = \int (dz)\, \mathcal{F}_{4a} = \int (dz) \left[\frac{E_0 + C_0}{U^2 V} + \frac{N_0 + Z_0}{U^2 V^2} + \frac{N_1 + Z_1}{U^3 V} \right]$$

where integrand and building blocks are given as follows:

$$\begin{aligned}
(dz) &= dz_1 dz_2 dz_3 dz_4 dz_5 \delta(1 - z_{12345}) \\
B_{11} &= z_{235},\ B_{12} = z_{35},\ B_{13} = -z_2, \\
B_{23} &= z_{14},\ B_{22} = z_{1345},\ B_{33} = z_{124}, \\
U &= z_2 B_{12} + z_{14} B_{11}, \\
A_i &= 1 - (z_1 B_{1i} + z_2 B_{2i} + z_3 B_{3i})/U, \\
G &= z_1 A_1 + z_2 A_2 + z_3 A_3,\ V = z_{123} - G, \\
z_{ijk\dots} &= z_i + z_j + z_k + \cdots .
\end{aligned}$$

$$\begin{aligned}
E_0 &= 8(2A_1A_2A_3 - A_1A_2 - A_1A_3 - A_2A_3) \\
C_0 &= -24 Z_4 Z_5 / U \\
N_0 &= G(E_0 - 8(2A_2 - 1)) \\
Z_0 &= 8z_1(-A_1 + A_2 + A_3 + A_1A_2 + A_1A_3 - A_2A_3) \\
&\quad +8z_2(1 - A_1A_2 + A_1A_3 - A_2A_3 + 2A_1A_2A_3) \\
&\quad +8z_3(A_1 + A_2 - A_3 - A_1A_2 + A_1A_3 + A_2A_3) \\
N_1 &= 8G(B_{12}(2 - A_3) + 2B_{13}(1 - 2A_2) + B_{23}(2 - A_1)) \\
Z_1 &= -8z_1(B_{12}(1 - A_3) + B_{13} + B_{23}A_1) \\
&\quad +8z_2(B_{12}(1 - A_3) - 4B_{13}A_2 + B_{23}(1 - A_1)) \\
&\quad -8z_3(B_{12}A_3 + B_{13} + B_{23}(1 - A_1))
\end{aligned}$$

Step 3: UV subtraction

- M_{4a} is not well-defined — it has UV divergences when the loop momenta goes to infinity.
- This corresponds to a region of z_i's when all z_i on the loop vanish simultaneously.
- We prepare an integral which has the same UV divergent profile by K-operation, and perform subtraction point-by-point on the integrand.

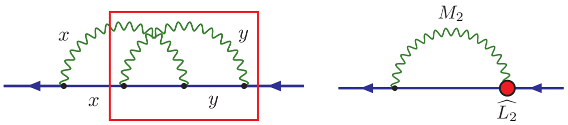

$\mathcal{F}_{M_{4a}}$ $\qquad$ $\mathbb{K}_{23}\mathcal{F}_{M_{4a}}$

- Then the finite part of the anomalous magnetic moment ΔM_{4a} is obtained by the integral:

$$\Delta M_{4a} = \int (dz) \left[\mathcal{F}_{4a} - \mathbb{K}_{12}\mathcal{F}_{4a} - \mathbb{K}_{23}\mathcal{F}_{4a} \right]$$

Step 4: IR subtraction

- M_{4b} has IR divergence as well, from vanishing of virtual photon momentum.
- This logarithmic IR divergence is handled by an integral which is constructed by I-subtraction.
- Then the finite part of the anomalous magnetic moment ΔM_{4b} is obtained by the integral:

$$\Delta M_{4b} = \int (dz) \left[\mathcal{F}_{4b} - \mathbb{K}_{22}\mathcal{F}_{4b} - \mathbb{I}_{13}\mathcal{F}_{4b} \right]$$

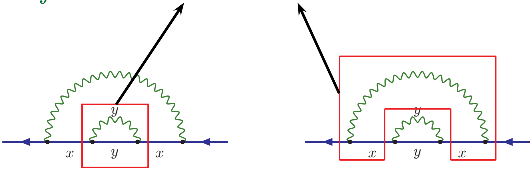

Step 5: Residual renormalization

- Finite part of amplitude is given in terms of integral with appropriate UV and/or IR subtraction terms.

$$\Delta M_{4a} = \int (dz) \left[\mathcal{F}_{4a} - \mathbb{K}_{12}\mathcal{F}_{4a} - \mathbb{K}_{23}\mathcal{F}_{4a} \right]$$
$$= M_{4a} - \widehat{L}_2 M_2 - \widehat{L}_2 M_2$$

$$\Delta M_{4b} = \int (dz) \left[\mathcal{F}_{4b} - \mathbb{K}_{22}\mathcal{F}_{4b} - \mathbb{I}_{13}\mathcal{F}_{4b} \right]$$
$$= M_{4b} - (\delta m_2 M_{2^\star} + \widehat{B}_2 M_2) - \widetilde{L}_2 M_2$$

- Subtraction terms are analytically factorized into products of lower-order quantities.
- Standard on-shell renormalization is denoted by

$$a^{(4)}[\text{q-type}] = M_{4a} - 2L_2 M_2 + M_{4b} - (\delta m_2 M_{2^\star} + B_2 M_2)$$

- By substitution, magnetic moment is given

$$a^{(4)}[\text{q-type}] = (\Delta M_{4a} + \Delta M_{4b}) - \Delta LB_2 \; M_2$$

where ΔLB_2 is finite part of $L_2 + B_2$.

Amplitude as a finite integral

- Finite amplitude $\Delta M_{\mathcal{G}}$ free from both UV and IR divergences is obtained by Feynman-parameter integral as:

$$\Delta M_{\mathcal{G}} = \int (dz) \Big[F_{\mathcal{G}}$$

← unrenormalized amplitude

$$+ \sum_{f} \prod_{\mathcal{S} \in f} (-\mathbb{K}_{\mathcal{S}}) F_{\mathcal{G}}$$

← UV subtraction terms

f: **Zimmermann's forests**:
combinations of UV divergent subdiagrams.

$$+ \sum_{\tilde{f}} (-\mathbb{I}_{\mathcal{S}_i}) \cdots (-\mathbb{R}_{\mathcal{S}_j}) \cdots F_{\mathcal{G}} \Big]$$

← IR subtraction terms

$\tilde{f}$: **annotated forests**:
combinations of self-energy subdiagrams
with distinction of I-/R-subtractions.

Residual renormalization

- We adopt the standard on-shell renormalization to ensure that the coupling constant α and the electron mass m_e are the ones measured by experiments.
- The sum of all these finite integrals defined by K-operation and I-/R-subtraction operations does not correspond to physical contribution to $g-2$.
- The difference is adjusted by the step called the residual renormalization.

$$
\begin{aligned}
a_e &= M(\text{bare}) - \text{on-shell renormalization} \\
&= \underbrace{\Big[M(\text{bare}) - \text{UV subtr.} - \text{IR subtr.}\Big]}_{\text{Finite integral } \Delta M} \\
&\quad + \underbrace{\Big[-\text{on-shell renorm.} + \text{UV subtr.} + \text{IR subtr.}\Big]}_{\text{finite residual renormalization}}
\end{aligned}
$$

Deriving residual renormalization

- Sum up over 389 integrals of 10th order Set V, which requires analytic sum of $\sim$ 16,000 symbolic terms.
- The physical contribution from 10th order Set V is given as:

$$
\begin{aligned}
A_1^{(10)}[\text{Set V}] = {} & \Delta M_{10}[\text{Set V}] \\
& + \Delta M_8(-7\Delta LB_2) \\
& + \Delta M_6\{-5\Delta LB_4 + 20(\Delta LB_2)^2\} \\
& + \Delta M_4\{-3\Delta LB_6 + 24\Delta LB_4\Delta LB_2 - 28(\Delta LB_2)^3 + 2\Delta L_{2*}\Delta dm_4\} \\
& + M_2\{-\Delta LB_8 + 8\Delta LB_6\Delta LB_2 - 28\Delta LB_4(\Delta LB_2)^2 \\
& \qquad + 4(\Delta LB_4)^2 + 14(\Delta LB_2)^4 + 2\Delta dm_6\Delta L_{2*}\} \\
& + M_2\Delta dm_4(-16\Delta L_{2*}\Delta LB_2 + \Delta L_{4*} - 2\Delta L_{2*}\Delta dm_{2*}),
\end{aligned}
$$

- The terms with Δ are the finite nth order quantities.
  - ΔM_n, M_2: finite magnetic moment.
  - ΔLB_n: sum of vertex and wave-function renormalization constants.
  - Δdm_n: mass-renormalization constants.
  - ΔL_n^*, Δdm_n^*: $*$ denotes mass insertion.

Construction of numerical integration code

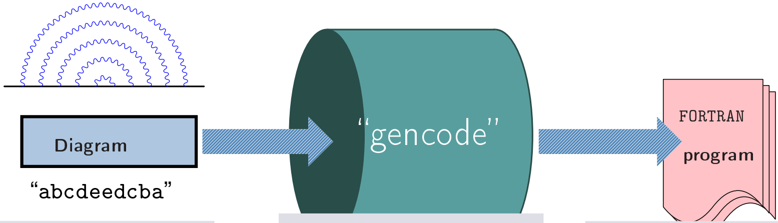

Symbolic representation of diagram

Build Amplitude,
Identify divergences,
Construct subtraction terms

Numerical integration code

- We need to evaluate a large number of Feynman diagrams.
  It should be error-prone by writing numerical integration code for these huge integrals by hand. We developed an automated code-generating program.
- "gencode*N*" takes a single-line information that represents a diagram, and generates numerical integration code in FORTRAN.
- These integrals are evaluated on computers using numerical integration routines.

AHKN, NPB740, 138 (2006); NPB796, 184 (2008)

Numerical integration

- Multi-dimensional integral
  - The amplitude is expressed as a $14-1$ dimensinal integral for 10th order diagrams.
  - The integrands are huge. (approx. $\mathcal{O}(10^5)$ FORTRAN lines for each integral.)
- Digit-deficiency problem
  - The point-by-point subtraction suffers from severe digit-deficiency problem by rounding-off of floating-point numbers.

    We employ extended numerical precision arithmetic using *double-double* and *quadruple-double* of `qd` library.

    Bailey, Hida, Li. c.f. http://crd.lbl.gov/˜dhbailey/mpdist/
- Sharp peaks
  - Integrands have sharp peaks due to divergences, and therefore requires robust integration method.

    We employ VEGAS, an adaptive-iterative Monte-Carlo integration algorithm.

    Lepage, J.Comput.Phys.27, 192 (1978)
    A new version of VEGAS: https://github.com/gplepage/vegas

Numerical checks of Set V integrals

- 13 integration variables in $[0,1]^D$ are mapped to 14 Feynman parameters. Any mapping should yield the same result.
- As a cross check, we performed integrals with different mappings. They are regarded as independent evalations.
- Numerical results are in good agreement.

List of results that exhibit relatively large differences:

Diagram	Expression	Results in 2015	Results in 2017	Difference	Weighted average
$X141$	$abbcadedec$	-12.5567 (350)	-12.4879 (207)	-0.0688	-12.5057 (178)
$X113$	$abacddeebc$	-4.3847 (322)	-4.4412 (176)	0.0565	-4.4282 (155)
$X100$	$abacdcdeeb$	-15.2919 (331)	-15.2360 (203)	-0.0559	-15.2513 (173)
$X256$	$abccdeedba$	-14.0405 (342)	-13.9856 (194)	-0.0549	-13.9990 (169)
$X146$	$abbcdadeec$	-2.2990 (335)	-2.2458 (202)	-0.0532	-2.2600 (173)
$X075$	$abacbddeec$	-8.1138 (340)	-8.0608 (195)	-0.0531	-8.0739 (169)
$X144$	$abbccdedea$	23.7239 (368)	23.6713 (189)	0.0526	23.6823 (168)
$X252$	$abccdedeab$	-10.9091 (343)	-10.8565 (179)	-0.0526	-10.8677 (158)
$X236$	$abcbdedcea$	2.0560 (180)	2.1072 (205)	-0.0512	2.0782 (135)
$X325$	$abcdceedba$	11.5958 (343)	11.5456 (198)	0.0503	11.5582 (172)
$X158$	$abbcdeceda$	0.4607 (329)	0.4106 (206)	0.0502	0.4247 (174)

AKN, PRD97, 036001 (2018)

12th order contribution?

- There are 202,770 vertex Feynman diagrams contributing to 12th order. The Feynman-parametric integral involves 16 dimensional numerical integration, each combinatorially more complicated than those of 10th order.
- Consider that $\left(\frac{\alpha}{\pi}\right)^6 \sim O(10^{-16})$, and the present uncertainty of a_e is of $O(10^{-13})$, it is not likely that 12th-order contribution is needed for the time being.
- In view of rather large values of $A_2(m_\mu/m_e)$ for muon $g-2$, one might wonder how much the twelfth order contribution.
- The leading contribution will come from three insertions of 2nd-order vacuum-polarization loop into the 6th-order light-by-light diagram. It is estimated as:

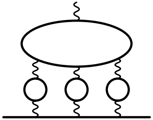

$$\sim \text{(6th light-by-light)} \times \text{(2nd VP)}^3 \times 10 \times \left(\frac{\alpha}{\pi}\right)^6$$

$$\sim 0.08 \times 10^{-11}.$$

It is larger than the uncertainty of 10th order term. A crude evaluation may be desirable.

Fine Structure Constant α from a_e

- From the measurement and the theory of electron $g-2$, the value of fine-structure constant can be determined.

Theoretical calculations

Experimental value

$$a_e = A^{(2)}\left(\frac{\alpha}{\pi}\right) + A^{(4)}\left(\frac{\alpha}{\pi}\right)^2 + A^{(6)}\left(\frac{\alpha}{\pi}\right)^3 + A^{(8)}\left(\frac{\alpha}{\pi}\right)^4 + A^{(10)}\left(\frac{\alpha}{\pi}\right)^5 + \cdots$$

$+$(small contributions)

- Newly obtained value of fine-structure constant is: (α^5) (had) (exp)

$$\alpha^{-1}(a_e) = 137.035\,999\,1496\,(13)(14)(330) \quad [0.24\text{ppb}]$$

AKN, Atoms, 7, 28 (2019)

- The differences in α from the atomic recoil determinations are

$$\alpha^{-1}(a_e) - \alpha^{-1}(\text{Rb}) = 0.155\,(91) \times 10^{-6}\ [1.7\sigma],$$
$$\alpha^{-1}(a_e) - \alpha^{-1}(\text{Cs}) = 0.104\,(43) \times 10^{-6}\ [2.4\sigma].$$

Summary

- QED contribution to electron $g-2$ up to 8th order has been firmly established. The 10th order term has been evaluated by extensive numerical calculation.
- QED contributions are now ready for the on-going new measurements of electron and position $g-2$, and muon $g-2$.
- Electron $g-2$ provides one of most precise determinations of fine structure constant α.
- With the improved value of the fine-structure constant α, it seems that a small discrepancy between the measurement and the theory of electron $g-2$ may be reveiled. Whether it is significant or not will wait for further improvements.